



Tilt angles for optimizing energy reception by fixed and periodically adjusted solar-irradiated surfaces in Nigeria

H. O. Njoku^{1,2} · U. G. Azubuike¹ · E. C. Okoroigwe¹ · O. V. Ekechukwu¹

Received: 23 December 2019 / Accepted: 24 April 2020 / Published online: 11 June 2020
© Islamic Azad University (IAU) 2020

Abstract

The insolation received on a solar collecting surface is maximized by ensuring the beam component of solar radiation which is normal to the surface. In this study, optimum tilt angles for fixed and periodically adjusted south-facing solar collecting surfaces have been estimated for different periods of the year, for locations in Nigeria (Lat. 4–14° N and Lon. 2–15° E). The spatial domain of interest was discretized into a grid of 1° latitude by 1° longitude cells; and for each cell, monthly average data of daily horizontal irradiation were obtained from the web-based NASA-SSE meteorological data services. These were used as inputs to an anisotropic tilt radiation model to search for the collector tilts that maximized incident radiation. A fixed collector tilt scheme and five periodic tilt angle adjustment schemes: adjustments of tilt angles (i) twice, (ii) thrice, (iii) four times, (iv) six times, and (v) twelve times in the year, were considered. Negative optimum tilt angles were obtained during the rainy season (April–August), indicating that for those periods, north-facing collector orientations will result in higher solar energy collection. Adjusting solar collectors twelve times per year, yielded the most annual irradiation, which was 3.4–6.7% more than the annual irradiation received by collectors with optimum angles fixed all year round. However, of the five periodic adjustment schemes, adjusting three times in the year is recommended as ideal, based on a comparison between the gains in the obtainable solar energy and the complexity/inconvenience associated with implementing the scheme.

Keywords Maximum insolation · Optimum tilt angle · Perez model · Solar radiation

Introduction

Solar collectors harness the inexhaustible solar radiation from the sun, and find applications in water heating, building heating, air conditioning, power generation, and industrial process heat. The angles to which these collectors are inclined with respect to the horizontal (i.e., their tilt angles) and the directions to which they are oriented greatly affect their performance and have appreciable effects on the quantities of received solar energy (Morcos 1994).

To harness maximum insolation, the radiation incident on a collector needs to be such that the beam radiation

component is dominant and normal to the collector's surface. This can be achieved with tracking mechanisms (single-axis and two-axes) set up to automatically track the sun's beam or position (Njoku 2016).

However, the trade-offs between the energy gains and the high (installation and maintenance) costs of these tracking mechanisms limit their usage (Oner et al 2009).

Alternatively, solar energy receiving surfaces can be fixed at optimal positions or intermittently adjusted to periodic optimal positions to maximize the solar energy received. For a periodically adjusted collector, as the number of intermittent adjustments of the collector to its optimum position is increased, the quantity of insolation which it receives would increase and approach the insolation that a tracking collector would harness (Notton and Diaf 2016). Compared to tracking collectors, the main advantages of solar collectors that are positioned at optimum tilt angles are cost effectiveness, ease of installation, and reduced maintenance.

The collector tilt angles that will maximize total insolation received can be determined experimentally, by employing pyranometers and solarimeters, but these

✉ H. O. Njoku
howard.njoku@unn.edu.ng; nwokoma@gmail.com

¹ Applied Renewable and Sustainable Energy Research Group, Department of Mechanical Engineering, University of Nigeria, Nsukka 410001, Nigeria

² Department of Mechanical Engineering Science, FEBE, University of Johannesburg, Auckland Park, Johannesburg 2006, South Africa

equipments are nominally installed to measure insolation on horizontal surfaces. Inclining them to the infinite number of possible tilt angles that will be required to determine the optimum will be practically unrealistic, necessitating a resort to modeling approaches. For these, numerous tilt radiation models have been developed, including isotropic or anisotropic models (Danandeh and Mousavi G. 2018; Gueymard and Ruiz-Arias 2016; Yadav and Chandel 2013; Yang 2016). Being more detailed in the analysis of the diffuse component of radiation, anisotropic models offer more accurate predictions of insolation (Li and Lam 2000; Khoo et al 2014), and numerous studies have shown that the Perez et al (1990) anisotropic model gives more accurate predictions in comparison to others (Elminir et al 2006; Noorian et al 2008; Gueymard and Ruiz-Arias 2016; Yang 2016).

Using the isotropic Liu and Jordan (1960) model, Ibrahim (1995) estimated the monthly, seasonal (when adjusted to four optimum tilts in a year), and annual optimum tilt angles of solar collectors in Guzelyurt Cyprus (Lat. 35° 11' N). While the annual β_{opt} was estimated as 31°, the seasonal β_{opt} were estimated as 22° in spring (Mar–May), 14° in summer (Jun–Aug), 40° in autumn (Sep–Nov.), and 48° in winter (Dec. to Feb.). The monthly β_{opt} varied between 52° in Dec. and 10° in June. Thus, the difference between monthly β_{opt} and location latitudes, L , ranged from 17° in winter to 42° in summer, while the annual $\beta_{opt} - L$ was $\sim 4^\circ$.

With the typical meteorological year as weather data input, Chow and Chan (2004) estimated the insolation received on inclined surfaces with different orientations and slopes, and for different periods of the year in Macau (22.2° N), South China. Annual β_{opt} of 25° ($\beta_{opt} - L = \sim 4^\circ$) and orientation of $\gamma = 40^\circ$ were suggested, while seasonal β_{opt} estimates were between 14° ($\beta_{opt} - L = \sim 8^\circ$) during summer and 45° ($\beta_{opt} - L = \sim 23^\circ$) during winter.

Bari (2000) developed a polynomial regression for estimating daily and seasonal β_{opt} for south-facing solar collectors in Malaysia (Lat. 1–7° N), based on the isotropic Liu and Jordan (1960) model. Sample computations for locations at latitudes 2.5° N, 3° N and 7° N, yielded both positive and negative β_{opt} depending on the season of the year. The negative β_{opt} implied that for certain periods of the year, collectors ought to be oriented towards the pole (rather than the equator) for optimized solar radiation collection. Alternatively, Nijegorodov et al (1994) developed linear correlations in the form of $\beta_{opt} = aL + b$ for calculating global monthly optimum tilt angles of south-facing solar collectors, with the location latitude, L , as the sole dependent variable, where a and b are constants that differ for the different months.

Elminir et al (2006) computed the optimum tilt angle that gave the maximum total radiation on collector surfaces

at Helwan (Lat. 29° 52' N and Lon. 31° 20' E) Egypt, based on the anisotropic Perez et al (1990) model. The β_{opt} was approximated as 43.33° during the winter season, 15° for the summer months, and 28.75° for collectors fixed throughout the year. These corresponded to $\beta_{opt} - L = \sim 14^\circ$, -14° and -1° , respectively. Similarly, for solar collectors in Syria (Lat. 34.8° N, Lon. 39° E), Skerker (2009) obtained β_{opt} that were approximately equal to the latitude for the months of March and September. The seasonal β_{opt} were estimated at 60° in winter, 19.34° in spring, 1.6° in summer, and 47° in autumn, while the yearly β_{opt} was estimated at 30.65°.

A number of studies for locations in Nigeria have also been reported. The study of Oladiran (1995) relied on the isotropic Liu and Jordan (1960) model and considered only three locations: Maiduguri (Lat. 11.8° N, Lon. 13.2° E), Ilorin (Lat. 8.5° N, Lon. 4.5° E), and Lagos (Lat. 6.4° N, Lon. 3.4° E) in Nigeria. Also, only three collector tilts ($\beta = L - 10^\circ$, L , and $L + 10^\circ$) were considered to obtain the results that suggested that during the dry season (between November and December) $\beta = L + 10^\circ$ gave the highest insolation at an azimuth angle of 0° for the three selected locations, while $\beta = L - 10^\circ$ was optimum during the rainy season. Idowu et al (2013) analyzed β_{opt} for solar heating collectors at locations within latitudes 1–14° in Nigeria, but based on insolation data for a 6.45° N location only. The β_{opt} obtained were predicted as $\beta_{opt} = L + 25^\circ$ for November, December, and January; $L + 15^\circ$ for February, September, and October; $L - 15^\circ$ for August; $L - 25^\circ$ for May, June, and July; and L for March and April.

Whereas the dependence of optimum collector tilt angles on location is established, the inherent diversity of the locations in Nigeria has not been adequately accounted for in the existing studies. In this paper, we undertook to determine the

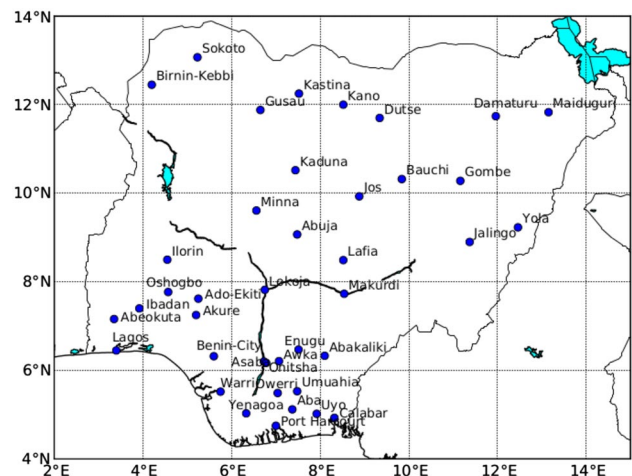


Fig. 1 The major cities in Nigeria (Njoku 2016)

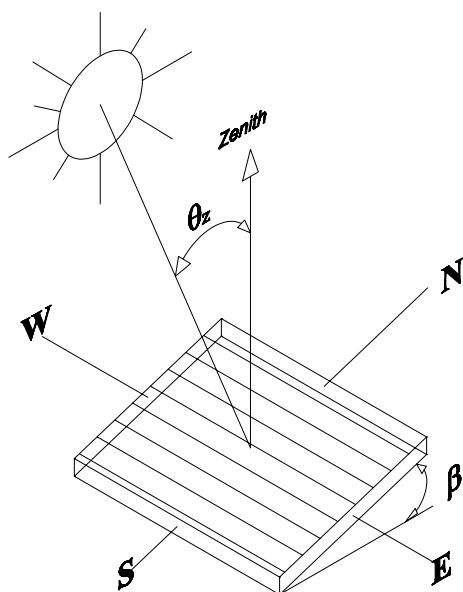


Fig. 2 Flat solar energy receiving surfaces in northern hemisphere with surface azimuth angle, $\gamma = 0^\circ$

optimum tilts of surfaces receiving solar radiation at locations on a 1° by 1° grid within latitudes $4\text{--}14^\circ$ N and longitudes $2\text{--}15^\circ$ E. Collector tilt adjustment schemes analyzed included surfaces fixed all year round and those periodically adjusted two, three, four, six, and twelve times per year. Data of monthly average daily insolation on horizontal surfaces, \bar{H} , were obtained from the NASA Surface Meteorology and Solar Energy (NASA-SSE) database (NASA-SSE 2016) and used for computing monthly insolation on surfaces inclined to different slopes based on the Perez et al (1990) model. The optimum tilt angles for solar radiation reception were determined by searching for the β values for which the total radiation on the collector surface was a maximum for the periods of interest or the entire year.

Materials and methods

Study domain

Figure 1 shows the study region which lies within latitudes $4\text{--}14^\circ$ N and longitudes $2\text{--}15^\circ$ E, encompassing all locations

in Nigeria and with major cities indicated with dots in the map. Locations in Nigeria are largely sub-equatorial and experience hot and humid climates with two distinct (rainy and dry) seasons. The annual average daily insolation levels are between 4.13 kWh/m^2 in the southernmost locations and 6.65 kWh/m^2 in the northernmost locations.

Tilt radiation model

Figure 2 depicts a flat south-facing solar energy collecting surface (orientation $\gamma = 0^\circ$) at a location in the northern hemisphere. The tilt angle, β , and zenith angle, θ_z are also indicated. According to the Perez et al (1990) model, the total average hourly insolation on such a surface, \bar{I}_T (J/m^2), is composed of beam, diffuse, and ground-reflected components. The average hourly beam insolation on a tilted surface, $\bar{I}_{T,b}$ (J/m^2), is the product of the average hourly beam radiation on the horizontal plane, \bar{I}_b , and a geometric factor, R_b , that is:

$$\bar{I}_{T,b} = \bar{I}_b R_b, \tag{1}$$

where R_b is the ratio of average hourly beam insolation on the tilted surface to that on a horizontal plane, given as:

$$R_b = \frac{\bar{I}_{T,b}}{\bar{I}_b} = \frac{\cos \theta}{\cos \theta_z}, \tag{2}$$

while \bar{I}_b is the difference between the average total (\bar{I}) and diffuse (\bar{I}_d) insulations on the horizontal plane; that is:

$$\bar{I}_b = \bar{I} - \bar{I}_d. \tag{3}$$

The diffuse component of the hourly irradiation on a horizontal surface, \bar{I}_d , was determined from the monthly average daily diffuse radiation, \bar{H}_d , by:

$$\bar{I}_d = r_d \bar{H}_d, \tag{4}$$

where, the ratio, r_d , is given by Liu and Jordan (1960) as:

$$r_d = \frac{\pi}{24} \frac{\cos \omega - \cos \omega_{ss}}{\sin \omega_{ss} - \frac{\pi \omega_{ss}}{180} \cos \omega_{ss}}, \tag{5}$$

with ω , the hour angle of the midpoint of the hour of interest, and ω_{ss} , the sunset hour angle. \bar{H}_d , the diffuse portion of \bar{H} , was obtained with the Erbs et al. correlations (Duffie and Beckman 2013), which express the ratio $R_d = \bar{H}_d/\bar{H}$, as a function of the hourly clearness index, K_T , as follows:

$$R_d = \begin{cases} 1.391 - 3.560\bar{K}_T + 4.189\bar{K}_T^2 - 2.137\bar{K}_T^3 & (\text{for } 0.25 \leq \bar{K}_T \leq 0.8; \omega_{ss} \leq 81.4) \\ 1.311 - 3.022\bar{K}_T + 3.427\bar{K}_T^2 - 1.821\bar{K}_T^3 & (\text{for } 0.25 \leq \bar{K}_T \leq 0.8; \omega_{ss} > 81.4), \end{cases} \tag{6}$$

where \bar{K}_T is the ratio of \bar{H} to \bar{H}_0 , the monthly average daily extra-terrestrial irradiation.

The average hourly diffuse component of the average hourly radiation on a tilted surface, $\bar{I}_{T,d}$ (J/m^2), is modeled by the Perez et al (1990) model as composed of the sum of isotropic ($\bar{I}_{T,d}^{\text{iso}}$), circumsolar ($\bar{I}_{T,d}^{\text{cs}}$), and horizon-brightening ($\bar{I}_{T,d}^{\text{hb}}$), sub-components, viz.:

$$\bar{I}_{T,d} = \bar{I}_{T,d}^{\text{iso}} + \bar{I}_{T,d}^{\text{cs}} + \bar{I}_{T,d}^{\text{hb}} \quad (7)$$

The isotropic diffuse sub-component, $\bar{I}_{T,d}^{\text{iso}}$, is given as:

$$\bar{I}_{T,d}^{\text{iso}} = \bar{I}_d(1 - F_1) \left(\frac{1 + \cos \beta}{2} \right), \quad (8)$$

where F_1 is the circumsolar coefficient; the circumsolar diffuse sub-component, $\bar{I}_{T,d}^{\text{cs}}$, is given by:

$$\bar{I}_{T,d}^{\text{cs}} = \bar{I}_d F_1 \frac{a}{b} \quad (9)$$

where a and b are sky geometric parameters, while the horizon-brightening diffuse sub-component, $\bar{I}_{T,d}^{\text{hb}}$, is given by:

$$\bar{I}_{T,d}^{\text{hb}} = \bar{I}_d F_2 \sin \beta, \quad (10)$$

where F_2 is the horizon brightness coefficient.

The average hourly ground reflected component of the radiation on a tilted surface, $\bar{I}_{T,g}$ (J/m^2), is given as:

$$\bar{I}_{T,g} = \bar{I}_d \rho_g \left(\frac{1 - \cos \beta}{2} \right), \quad (11)$$

where ρ_g is the ground albedo.

Summing Eqs. (1), (8), (9), (10), and (11), the total average hourly insolation on a tilted surface is given by the Perez et al (1990) model as:

$$\begin{aligned} \bar{I}_T = & \bar{I}_b R_b + \bar{I}_d(1 - F_1) \left(\frac{1 + \cos \beta}{2} \right) + \bar{I}_d F_1 \frac{a}{b} \\ & + \bar{I}_d F_2 \sin \beta + \bar{I}_d \rho_g \left(\frac{1 - \cos \beta}{2} \right). \end{aligned} \quad (12)$$

Tilt angle optimization scheme

Data of monthly and average daily insolation on horizontal surfaces, \bar{H} and \bar{H}_{ann} , respectively, were provided by the web-based NASA-SSE database (NASA-SSE 2016) as one of over 200 satellite-derived monthly meteorological and solar energy parameters averaged over 22 years and covering the entire surface of the earth on a 1° by 1° grid. These data, whose accuracies have been assessed by Elminir et al (2006), Kawajiri et al (2011), Zawilska and Brooks (2011), Ghosh et al (2010), etc., were obtained and decomposed using the

Collares-Pereira and Rabl (1979) equations to obtain the hourly \bar{I} values used in Eqs. (1)–(12). (Details of the procedure are presented in Njoku (2016)).

Prediction of optimum tilt angles for surfaces fixed all year round

The optimum tilt angles, β_{opt} , were determined for surfaces fixed all year round following the steps outlined in the flow-chart of Fig. 3. For each cell in the 1° by 1° grid for which NASA-SSE data were obtained, the optimization process began with the collector tilt, β , set equal to the location's latitude L and the maximum annual radiation, $\bar{H}_{T,ann}^{\text{max}}$, set to the \bar{H}_{ann} that was obtained from the NASA-SSE database. Using the \bar{H} value for each month, the total radiation received by a surface inclined at β was computed for each day of the month, using Eqs. (1)–(12) and summed to obtain the total radiation on the inclined surface for the month, \bar{H}_T . This was repeated for the 12 months of the year. Then, the total monthly irradiations were summed to obtain the total annual irradiation received by the tilted surface $\bar{H}_{T,ann}$. The $\bar{H}_{T,ann}$ was then compared with the $\bar{H}_{T,ann}^{\text{max}}$, and if $\bar{H}_{T,ann}$ was greater, then $\bar{H}_{T,ann}^{\text{max}}$ was updated to be equal to $\bar{H}_{T,ann}$ and the procedure repeated with β increased by 0.5° . The procedure continued iteratively until a $\bar{H}_{T,ann}^{\text{max}}$ was obtained whose value was less than the latest $\bar{H}_{T,ann}$. The β values that gave the $\bar{H}_{T,ann}^{\text{max}}$ were taken as β_{opt} .

Prediction of optimum tilt angles for surfaces that are periodically adjusted

Five additional schemes were considered for periodically adjusting collector surfaces to periodic optimum tilt angles—two periodic adjustments (i.e., January–June and July–December); three periodic adjustments (i.e., January–April, May–August, and September–December), four periodic adjustments (i.e., January–March, April–June, July–September, and October–December), six periodic adjustments (i.e., January–February, March–April, May–June, July–August, September–October, and November–December), and 12 periodic adjustments (i.e., monthly).

The search procedures used for estimating the β_{opt} for each period of the five schemes were similar to that used in determining the β_{opt} for surfaces fixed all year round (Sect. 2.3.1) gave that the search algorithm sought the maximum irradiations on tilted surfaces during each period instead of the maximum annual irradiations. Furthermore, the starting β values were within the range of $L - 35^\circ \leq \beta \leq L + 40^\circ$, depending on the period of the year. The β values that gave the maximum irradiation for any period were taken as the β_{opt} for that period.

Fig. 3 Flowchart for the computations of β_{opt} for surfaces fixed all year round

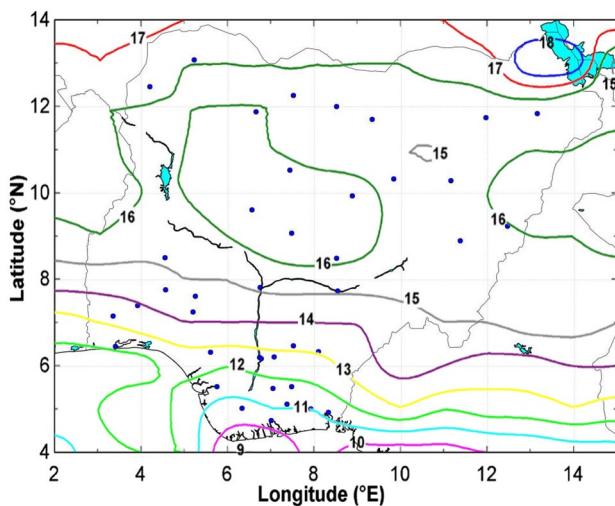
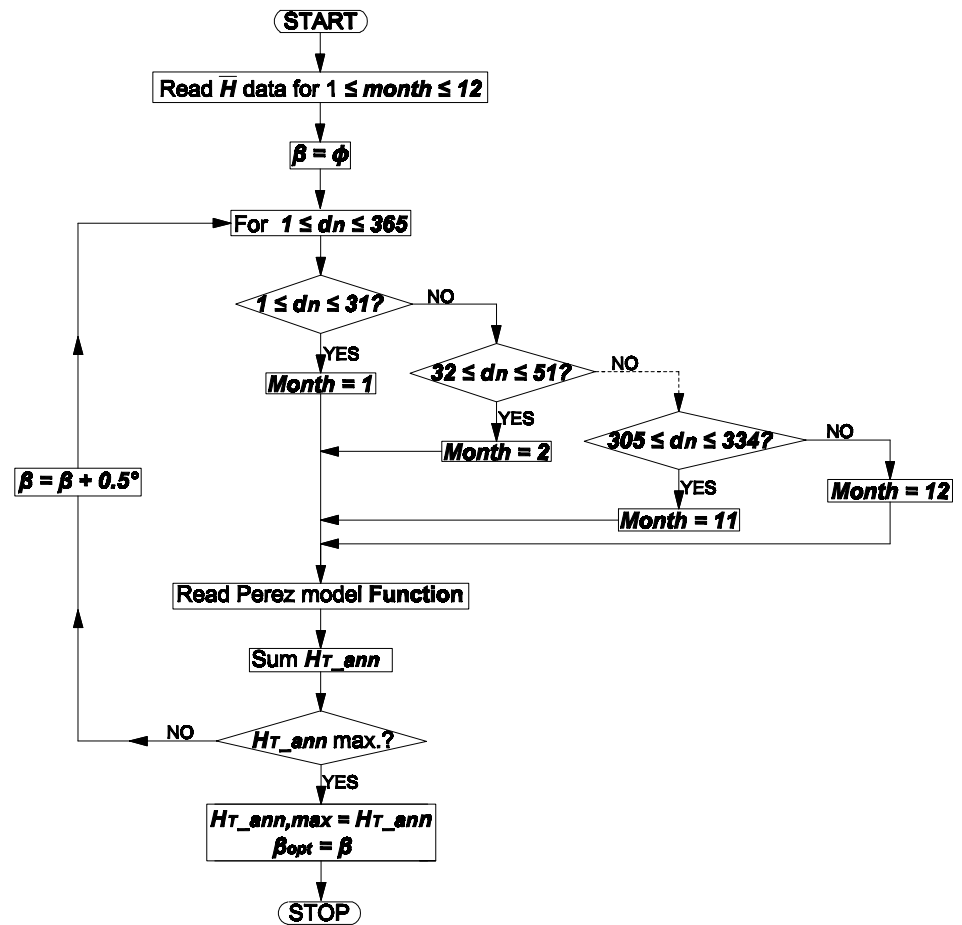


Fig. 4 Optimum tilt angles for optimally fixed surfaces in the study region

Results and discussion

Optimum tilt angles

Optimum tilt angle for surfaces optimally fixed all year round

Figure 4 shows isoclines of annual β_{opt} for optimally fixed surfaces within the study region. The dots on the figure represent the major locations earlier indicated in Fig. 1. It is evident, from Fig. 4, that the β_{opt} increase as location latitudes increase, with higher β_{opt} obtained for locations with higher latitudes. Thus, the southerly locations are less south-facing than the northerly locations. The least β_{opt} of $\sim 10^\circ$ was obtained for the southernmost Niger delta locations (within latitudes 4–5° N and longitudes 6–7° E), while the highest β_{opt} of $\sim 18^\circ$ was obtained at the north-easternmost locations, within the Lake Chad basin (latitudes 13–14° N and longitudes of 12–14° E).

The increase in β_{opt} with location latitudes is more pronounced at the southernmost areas, where β_{opt} increases by 6° (i.e., from 9° to 15°) between latitudes 4° and 8° N. However, within the central regions (between latitudes 8 and

12.5° N), surfaces can be practically fixed at a constant β_{opt} value of 16°, and at 17° for the northernmost locations to maximize solar energy collection. The values of β_{opt} shown in Fig. 4 are also generally close to the corresponding location latitudes; the $\beta_{\text{opt}} - L$ are between 3 and 6°.

Considering that the annual collected solar energy is not significantly altered by small changes in collector tilt—the annual captured solar energy changes by $\sim 0.2\%$ for each degree change in β (Lorenzo 2003)—these $\beta_{\text{opt}} - L$ values suggest that collector tilts equal to location latitudes will be a good approximation for optimizing solar energy collection by fixed surfaces in Nigeria. This agrees with the recommendation of Duffie and Beckman (2013) to keep surface tilts equal to the latitude for maximum annual energy availability, and most previous studies have obtained similar results (e.g., Yakup and Malik 2001; Tang and Wu 2004; Ng et al 2014; Ghosh et al 2010).

Optimum tilt angle for surfaces adjusted twice a year

For the case of two periodic adjustments of collector surfaces in a year, the β_{opt} for the January–June and the July–December periods are shown in Fig. 5a, b, respectively. For both periods, the β_{opt} trends are similar to the trends for the case of single annual optimum tilt (Fig. 4), with the β_{opt} varying from the least values at the southernmost locations to the highest values at the northernmost locations. The β_{opt} obtained for the January–June period ranges from 7.5° (at the extreme south) to 13.5° (at the extreme north), while for the July–December period, the range is from 12° to 22°. The increments in β_{opt} with location latitudes are also observed to be more pronounced for southern locations. In

the January–June period, β_{opt} increase by 4° between latitudes 4° and 8° N, and by $\leq 1.5^\circ$ for the rest of the study region; while in the July–September period, it increased by 8° and 3°, respectively.

The β_{opt} for the July–December period are higher than those for the January to June period. However, whereas the difference between the least β_{opt} values for the two periods is $\sim 1.1^\circ$, the highest β_{opt} values for the two periods differ by $\sim 4.5^\circ$. These differences represent the range of angular adjustments that have to be made to collectors at the end of each 6-month period to optimize irradiation on their surfaces. Obviously, these adjustments, whether small or large, will only be justified if they will result in significant improvements in energy collection. These angular adjustments also depend on the choice of the months composing each half-year period. For example, using half-year periods comprised of Jan–Jun and Jul–Dec, the end-of-period angular adjustment determined for Belgrade, Serbia (Lat. 44.78° N) by Despotovic and Nedic (2015) was 6.8°, while between the periods within 22 Mar–21 Sep and 22 Sep–21 Mar, the angular adjustment was obtained as 43.9°.

Optimum tilt angle for surfaces adjusted thrice a year

Due to the typical position of the sun with respect to terrestrial locations, the total insolation on a fixed solar irradiated surface is more when it is oriented towards the equator than when oriented away from the equator. This forms the basis for such general rules of thumb whereby collectors in the northern hemisphere are installed as south-facing, whereas those in the southern hemisphere are installed as north-facing (Duffie and Beckman 2013). Such rules are generally

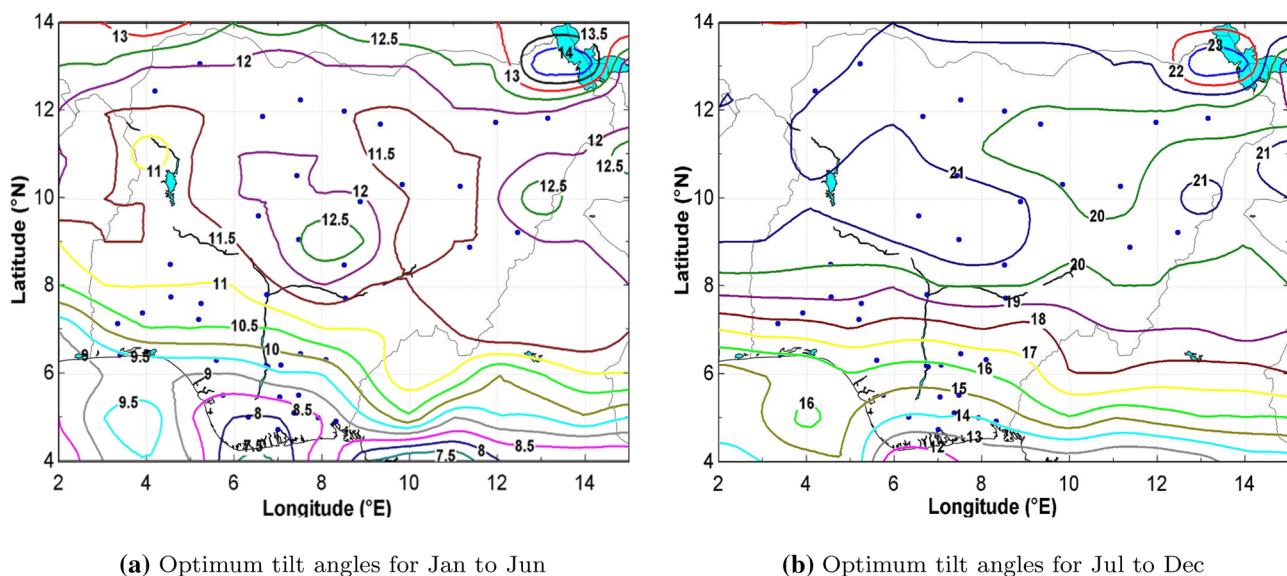


Fig. 5 Optimum tilt angles for surfaces adjusted within the study region twice a year

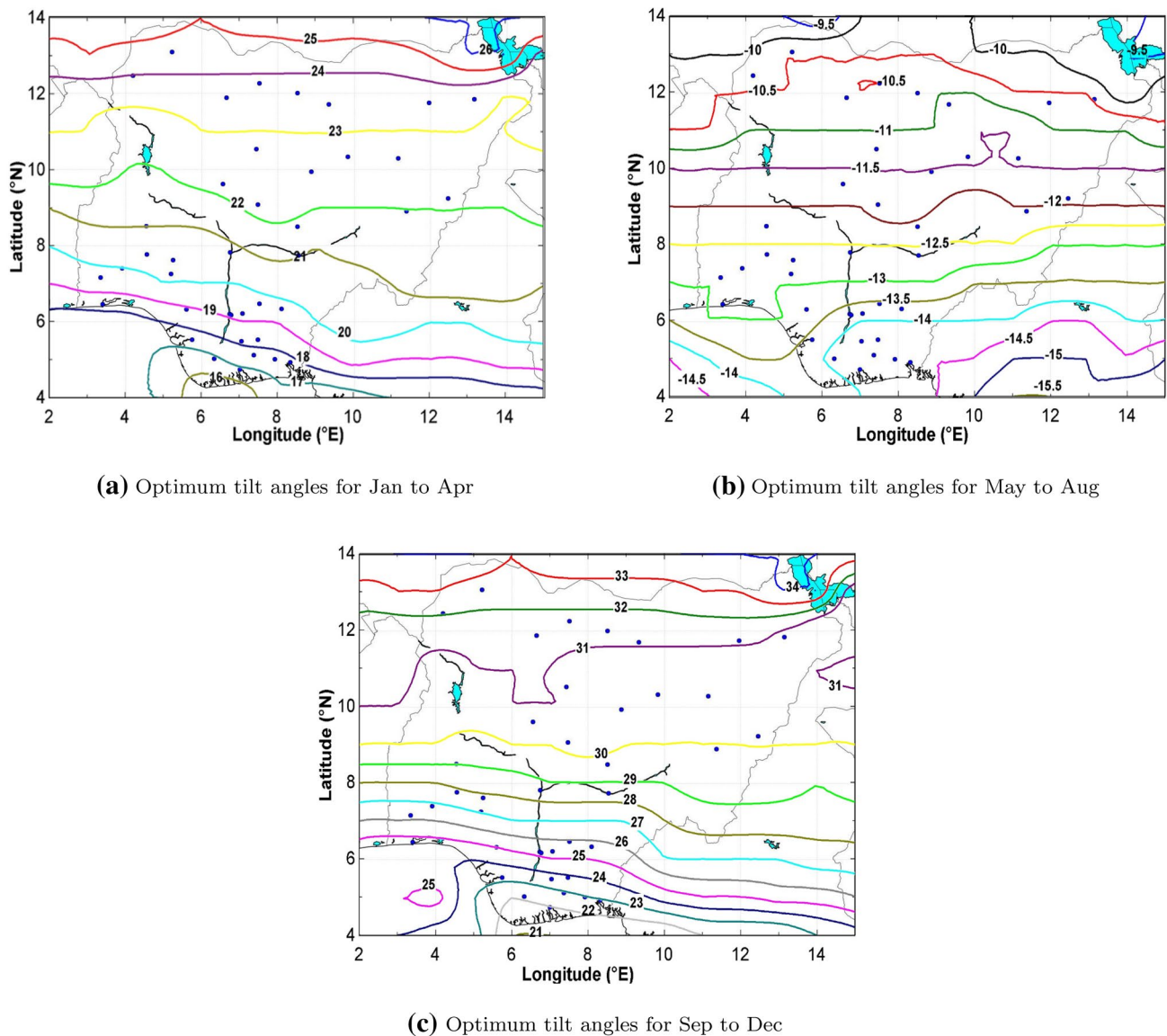


Fig. 6 Optimum tilt angles for surfaces within the study region adjusted thrice a year

true based on the analysis of beam radiation; but for specific locations, particularly those at low latitudes and which experience peculiar weather conditions, investigations such as the present one, establish the extent of validity of these generalizations (Chow and Chan 2004).

Figure 6 shows the β_{opt} for the case of surfaces adjusted to the optimum tilts corresponding to three periods of the year. Unlike the two previous cases, negative β_{opt} were obtained for the second period of the year (May–August, Fig. 6b). These negative β_{opt} mean that within this period, surfaces have to be oriented away from the equator (i.e., north-facing) to maximize solar energy collection.

The negative β_{opt} occur because on any day of the year that the solar declination is equal to a location's latitude, the

sun's beam radiation will be perpendicular to a horizontal collector at that location. However, on such a day, horizontal collectors at locations above that latitude will see the sun's beam radiation from the southerly direction, while locations below that latitude will see the sun beam radiation from a northerly direction. Surfaces at locations beneath the 23.45° N parallel (in the northern hemisphere) are most likely to experience this phenomenon as shown by the studies of Bari (2000), Ng et al (2014) and Yakup and Malik (2001), who obtained negative (north-facing) β_{opt} for Malaysia (Lat. 1–7° N), Bangi–Malaysia (Lat. 3° N), and Brunei Darussalam (Lat. 4.90° N), respectively, at certain periods of the year.

For further illustration, Fig. 7 shows how the solar declination angle varies during the year, with the latitudes 4 and

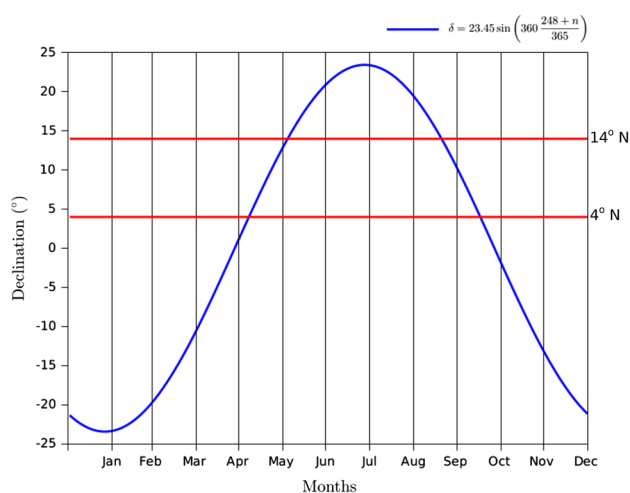


Fig. 7 Relationship between solar declination and periods of positive and negative β_{opt}

14° N (which bound the study region) indicated for illustration. At locations on the 4° N parallel, the solar declination is greater than 4° from early May to mid October, while for locations on the 14° N parallel, the solar declination is greater than 14° from early June to mid September. When the contributions of diffuse and ground-reflected radiations are included, during periods of the year approximately bounded by these months, collectors at these locations will have to be north-facing rather than south-facing as the common rule of thumb specifies for collectors in the northern hemisphere. The β_{opt} for the May–August period (Fig. 6b) corroborates this observation.

The positive β_{opt} values obtained for the January–April and the September–December periods are significantly greater than the β_{opt} values obtained in the fixed tilt and double adjustment cases. For these two periods, the β_{opt} values range within 16°–25° and 21°–34°, respectively, whereas for the May–August period, the β_{opt} range is –14.5° to –9.5°. Because of the increase in β_{opt} with latitude, solar irradiated surfaces in southerly locations will be more north-facing during the periods with negative β_{opt} (April–September) than those in the northerly locations.

Optimum tilt angle for surfaces adjusted four times a year

Figure 8 shows the β_{opt} for the case of surfaces that are adjusted to the optimum tilts corresponding to four periods of the year. While positive β_{opt} were obtained for the other two periods— January to March (Fig. 8a) and October–December (Fig. 8d), negative β_{opt} were obtained for two of the periods—April to June (Fig. 8b) and July–September (Fig. 8c). The β_{opt} obtained for the periods within April–September agree with the earlier deductions from

Fig 7. The latitudinal dependence of the β_{opt} values persists during the four periods, as β_{opt} values increase with location latitudes. However, except for the Oct–Dec period (Fig. 8c), the steep increases in β_{opt} at the southern locations, which were observed previously, are less pronounced.

Optimum tilt angle for surfaces adjusted twelve times a year

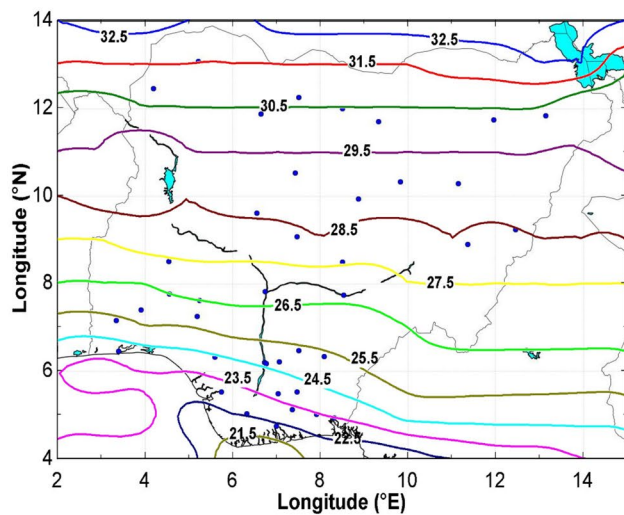
The β_{opt} that were obtained for surfaces adjusted to monthly optimum tilts are shown in Fig. 9. The β_{opt} are positive at all locations during the months of January–March and September–December, and negative between May and August. During the transition month of April, the β_{opt} values obtained are negative for northern locations in the study region but positive for southern locations. Consequently, if solar energy collecting surfaces within the study region are adjusted to monthly optimum tilts, their orientations will be south-facing during 7/8 months of the year but north-facing during 4/5 months of the year.

The maximum and minimum β_{opt} for each month are shown in Fig. 10. The plot shows that the monthly β_{opt} decline continuously from high positive (south-facing) values in January ($31^\circ \leq \beta_{\text{opt}} \leq 43^\circ$) till April, when collectors may practically be kept horizontal ($\beta_{\text{opt}} \approx 0$) to maximize solar energy collector. Thereafter, the β_{opt} become increasingly negative till June when collectors ought to be most north-facing ($-19^\circ \leq \beta_{\text{opt}} \leq -15^\circ$). Once again, β_{opt} increases continuously in the succeeding months, becoming positive again in September ($1^\circ \leq \beta_{\text{opt}} \leq 14^\circ$) and attains a maximum positive value in December ($33^\circ \leq \beta_{\text{opt}} \leq 45^\circ$).

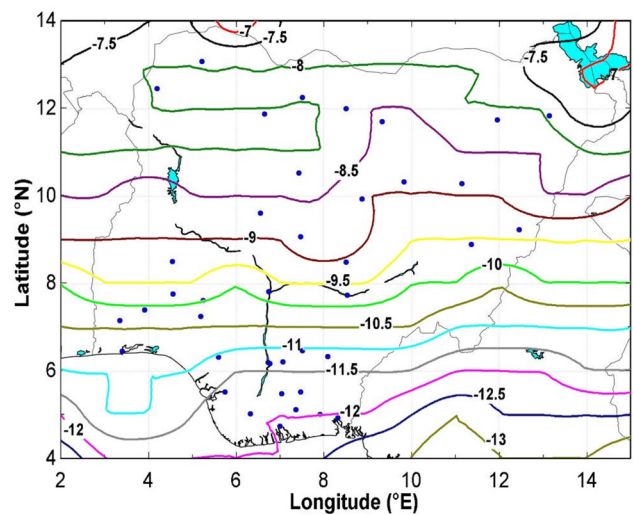
The correlations of Nijgorodov et al (1994) were used to calculate β_{opt} for six locations: Port Harcourt (Lat. 4.75° N), Nsukka (Lat. 6.52° N), Ilorin (Lat. 8.50° N), Kaduna (Lat. 10.52° N), Kano (Lat. 12.00° N), and Sokoto (Lat. 13.07° N), which represent the range location latitudes in Nigeria. These are compared in Table 1 with the results obtained in this study. A significant agreement is observed between the both sets of values, and the agreement is strongest for the dry seasons months (October–February). Marked deviations occur in the β_{opt} values for April–August, which coincide with the peak of the rainy season. During this period, the insolation received in these tropical locations is significantly affected by increased cloud cover, and this is not accounted for by the Nijgorodov et al (1994) correlations.

Latitude and location dependence of optimum tilt angles

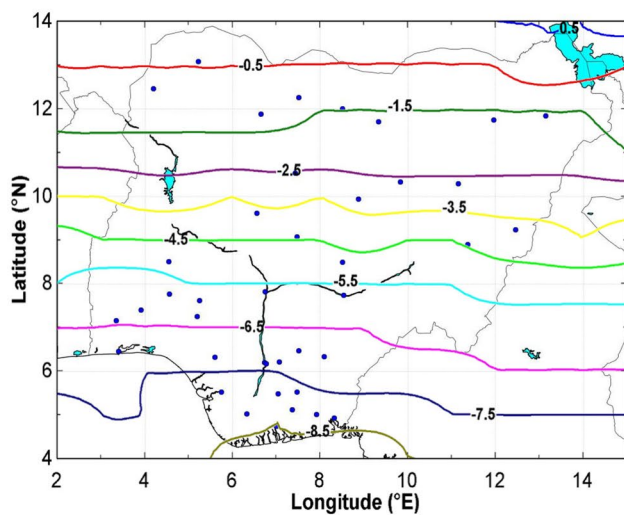
Figure 11 provides a graphical summary of the range of β_{opt} determined for the tilt adjustment schemes considered in this study. The corresponding $\beta_{\text{opt}} - L$ values are given



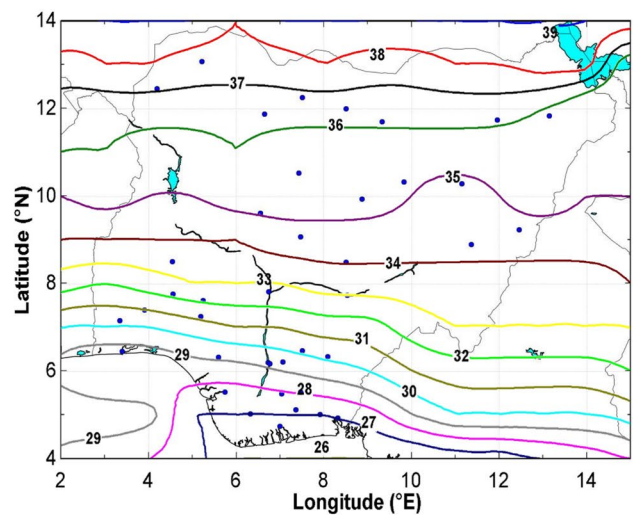
(a) Optimum tilt angles for Jan to Mar



(b) Optimum tilt angles for Apr to Jun



(c) Optimum tilt angles for Jul to Sep



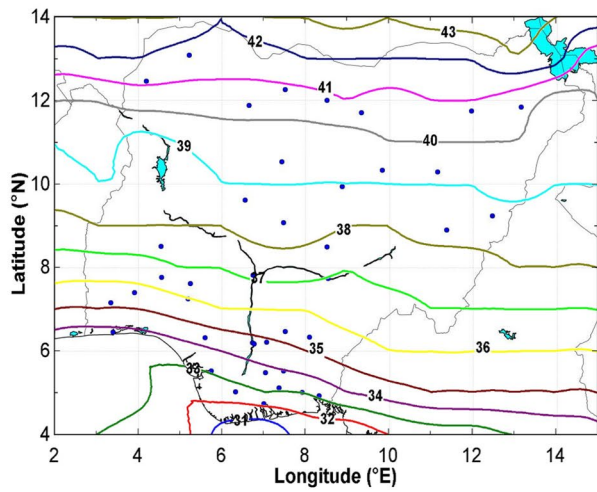
(d) Optimum tilt angles for Oct to Dec

Fig. 8 Optimum tilt angles for surfaces within the study region adjusted four times a year

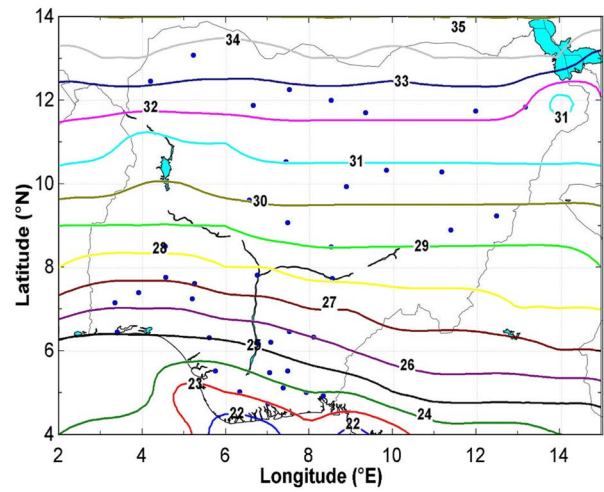
in Table 2. These β_{opt} values do not obey any single rule-of-thumb and their relationships with the location latitudes ($\beta_{opt} - L$) depend on the period of the year. For instance, for fixed case and for the first half of the year in the double yearly adjustments case, $\beta_{opt} \approx L$ will be a good approximation to maximize solar energy collection. For the second half of the year, however, $\beta_{opt} \approx L + 10^\circ$ will maximize solar energy collection. The other $\beta_{opt} - L$ values in Table 2 can be used for making decisions on appropriate collector inclinations for any location in Nigeria for maximizing solar energy collection based on any of the adjustment schemes.

Energy gains from optimum surface inclinations

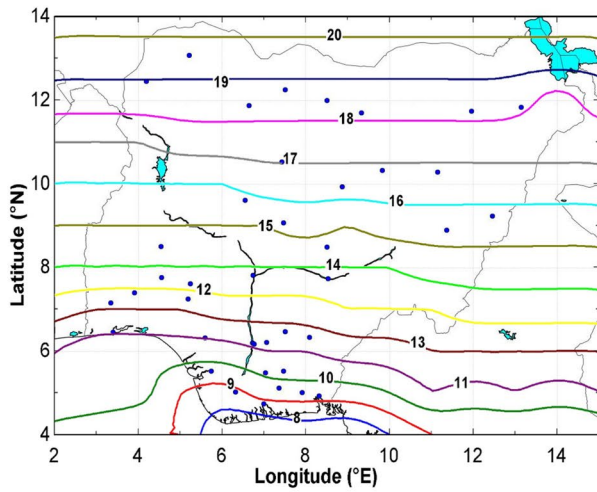
Figure 12a–f shows the total solar energy that is obtainable by collectors that are (a) fixed, or (b)–(f) subjected to 2–12 periodic adjustments in the year. As expected, higher solar energy gains were obtained for the northerly locations for all the collector tilt schemes, and the obtainable total solar energy progressively increases as the number of periodic tilt adjustments is increased. The obtainable energy with the fixed and periodic adjustment schemes is compared in Fig. 13, which shows the percentage gains in obtainable solar energy for the periodic adjustment schemes, above the



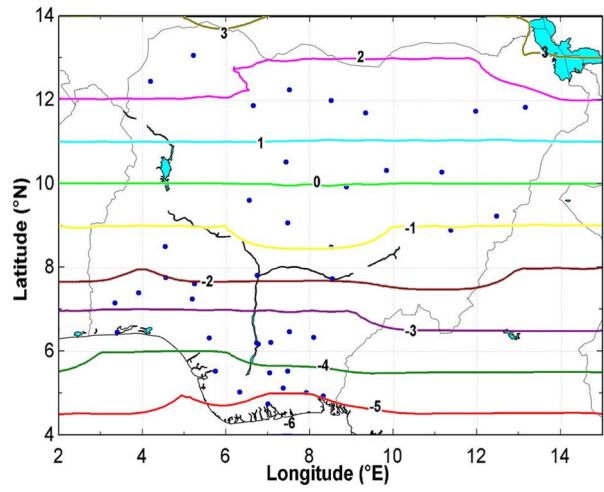
(a) Optimum tilt angles for January



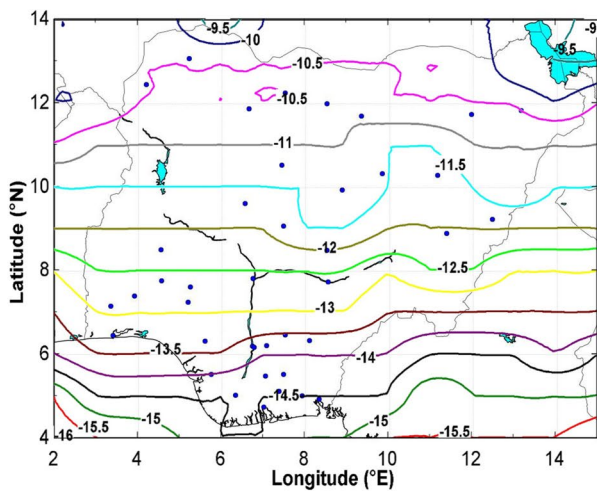
(b) Optimum tilt angles for February



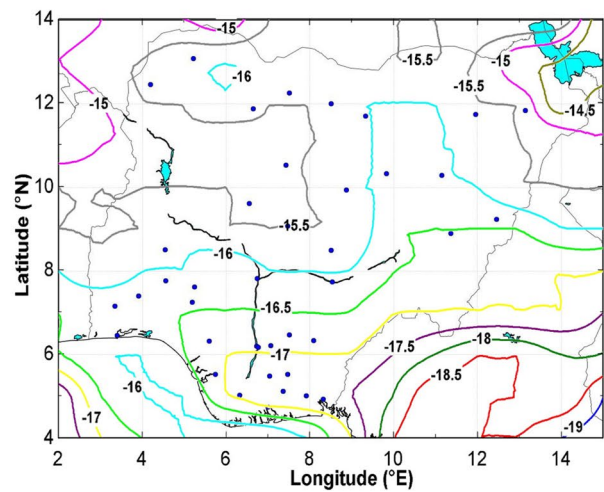
(c) Optimum tilt angles for March



(d) Optimum tilt angles for April

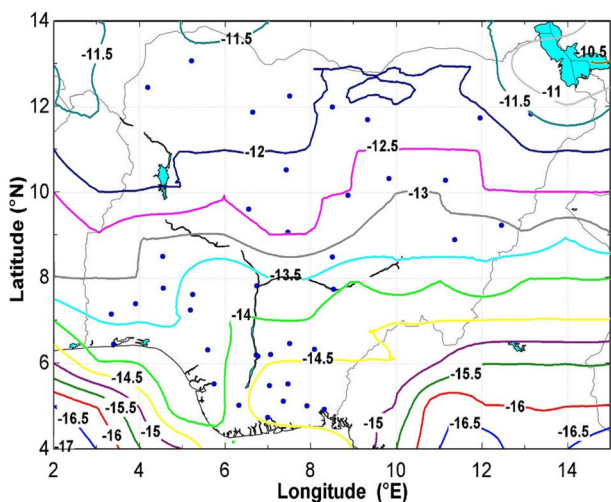


(e) Optimum tilt angles for May

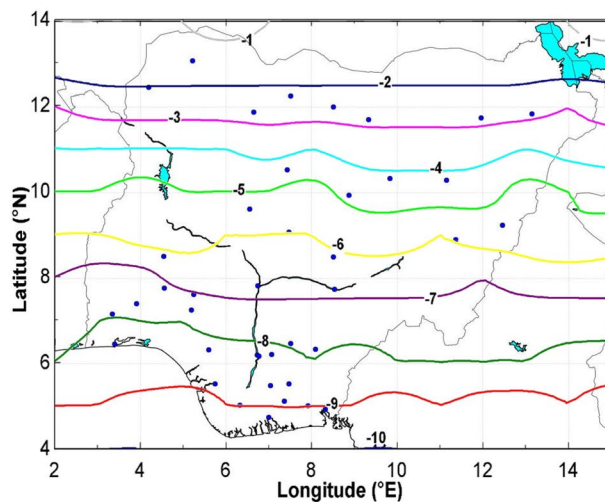


(f) Optimum tilt angles for June

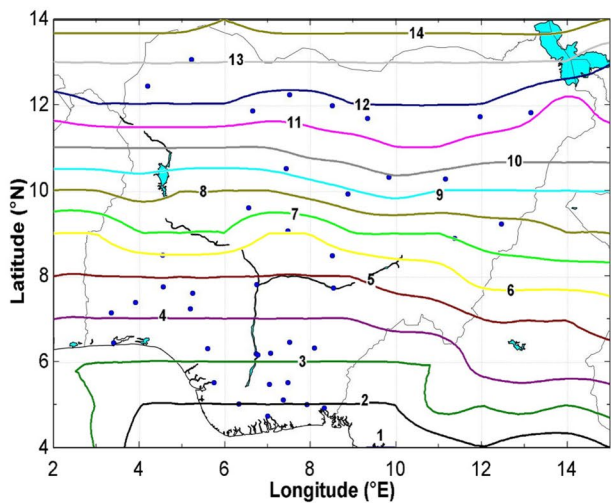
Fig. 9 Optimum tilt angles for the months of **a** January, **b** February **c** March, **d** April, **e** May, **f** June, **g** July, **h** August **i** September, **j** October, **k** November, and **l** December



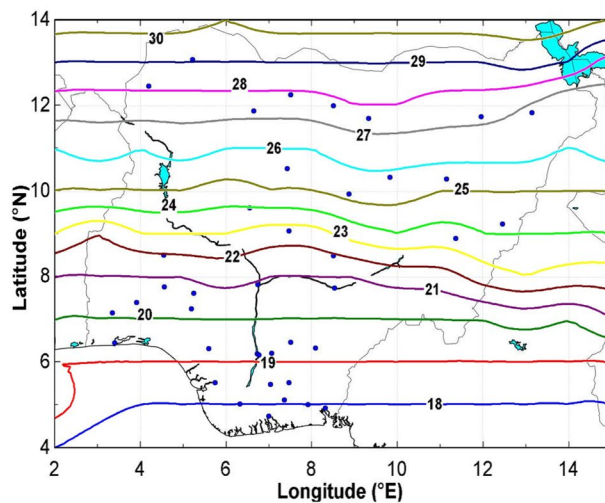
(g) Optimum tilt angles for July



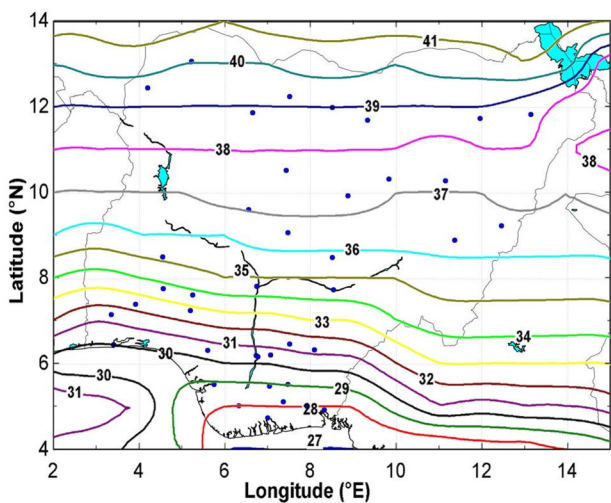
(h) Optimum tilt angles for August



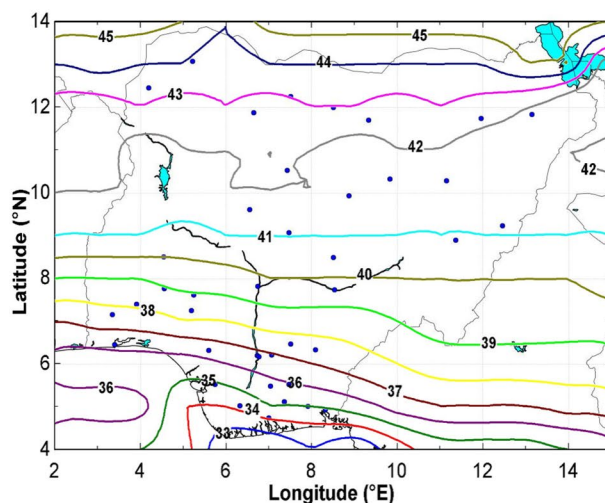
(i) Optimum tilt angles for September



(j) Optimum tilt angles for October



(k) Optimum tilt angles for November



(l) Optimum tilt angles for December

Fig. 9 (continued)

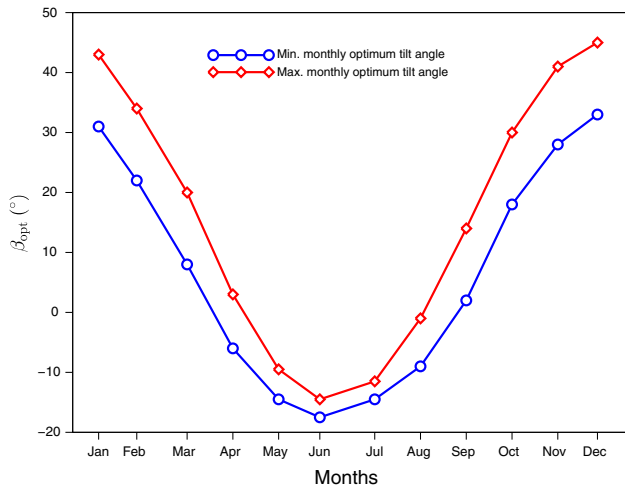


Fig. 10 Maximum and minimum monthly optimum tilt angles within the study domain

obtainable solar energy with the fixed scheme, χ . This is defined as:

$$\chi = \frac{\Sigma H_{ann}(\beta_{opt}) - \Sigma H_{ann}(\beta_{opt}^{fixed})}{\Sigma H_{ann}(\beta_{opt}^{fixed})} \times 100\%, \quad (13)$$

where $\Sigma H_{ann}(\beta_{opt})$ is the total annual irradiation obtainable with a scheme, while $\Sigma H_{ann}(\beta_{opt}^{fixed})$ is the total annual irradiation obtainable with the fixed scheme.

The monthly adjustment of collector tilts offers the highest gain in the obtainable solar energy beyond that of optimally fixed collectors, whereas the gain obtained by adjusting the collectors twice a year is insignificant. The choice of the number of tilt adjustments a year will clearly involve a trade-off between the gains in the obtainable energy and the complexity/inconvenience associated with implementing the periodic adjustments. The result of Fig. 13 suggests that adjusting collectors four times a year will be a reasonable compromise between the opposing considerations.

Conclusions

Optimum tilt angle for south-facing orientation for the study region has been determined for surfaces that are optimally: (i) fixed all year round, (ii) adjusted twice a year, (iii) adjusted thrice a year, (iv) adjusted four times a year, (v) adjusted six times a year, and (vi) adjusted twelve times a year. Fixed surfaces were found to have optimum tilt values that are close to the location latitudes. Hence, to maximize the solar energy obtainable by such collectors, their tilt angle may be fixed equal to the location latitude all year round.

For the periodically adjusted collectors, negative optimum tilt angles were obtained for periods within the rainy season (April–August), which largely coincide with the period when the solar declination is greater than the latitudes of the locations studied. Thus, to maximize the obtainable solar energy, collectors within the study locations should be

Table 1 Comparison of optimum tilt angles (β_{opt}) of south-facing collectors ($\gamma = 0$) calculated in this study and using the correlations of Nijegorodov et al (1994) at selected location in Nigeria

	Months											
	Jan	Feb	Mar	Apr	May	Jun	Jul	Aug	Sep	Oct	Nov	Dec
Port Harcourt (Lat. 4.75° N)												
Present study	30	21.5	7	-6	-14.5	-15.5	-14	-9.5	1	17	27	32
Nijegorodov et al (1994)	33.2	21.6	8.8	-5.2	-19.6	-29.9	-25.8	-12.4	2.8	16.8	29.4	38.1
Nsukka (Lat. 6.52° N)												
Present study	35	25.5	11.5	-3	-13.5	-16.5	-14	-8	3.5	19.5	31	37.5
Nijegorodov et al (1994)	34.8	23.3	10.5	-3.5	-17.9	-28.3	-24.2	-10.7	4.5	18.5	31.1	39.7
Ilorin (Lat. 8.50° N)												
Present study	36.5	27.5	14	-2	-12.5	-16	-13	-7.5	5	21	34	39
Nijegorodov et al (1994)	36.6	25.2	12.5	-1.5	-16.1	-26.6	-22.4	-8.8	6.5	20.5	32.9	41.4
Kaduna (Lat. 10.52° N)												
Present study	39	30.5	16.5	0	-11.5	-15.5	-12	-5	8	25	37.5	42
Nijegorodov et al (1994)	38.4	27.2	14.5	0.5	-14.2	-24.8	-20.6	-6.8	8.5	22.5	34.8	43.2
Kano (Lat. 12.00° N)												
Present study	40.5	32.5	18.5	1.5	-10.5	-15.5	-12	-2.5	11.5	27.5	39	43
Nijegorodov et al (1994)	39.7	28.6	16.0	2.0	-12.8	-23.6	-19.3	-5.4	10.0	24.0	36.2	44.4
Sokoto (Lat. 13.07° N)												
Present study	41.5	33.5	19.5	2.5	-10.5	-16	-11.5	-1.5	13	29	40	44
Nijegorodov et al (1994)	40.6	29.7	17.1	3.1	-11.8	-22.6	-18.4	-4.3	11.1	25.1	37.2	45.4

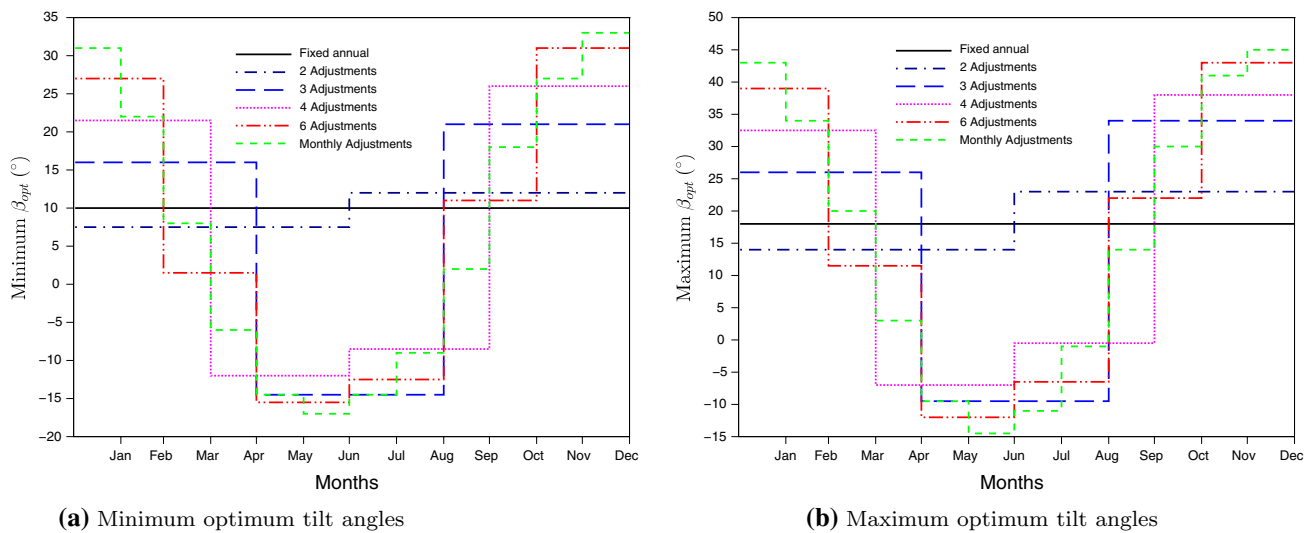


Fig. 11 Maximum and minimum optimum tilt angles for the different tilt adjustment schemes

Table 2 Difference between optimum tilt angles and location latitudes ($\beta_{opt} - L$) for fixed and periodic collector adjustment schemes

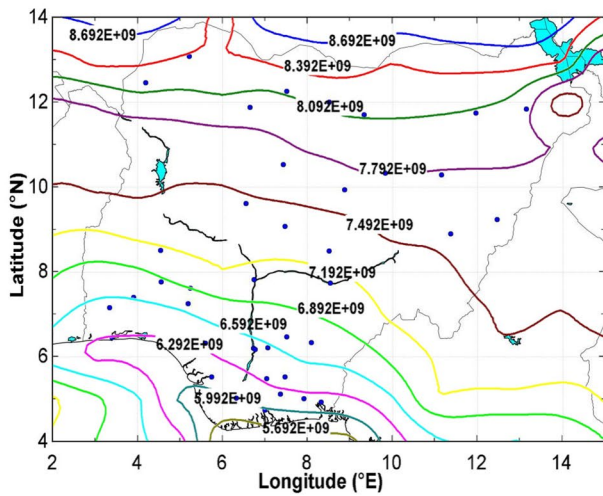
Months	$\beta_{opt} - L$ (°)											
	Fixed		2 periods		3 periods		4 periods		6 periods		Monthly	
	Min.	Max.	Min.	Max.	Min.	Max.	Min.	Max.	Min.	Max.	Min.	Max.
January	3	6	-0.5	3.5	12	12	17.5	18.5	23	25	28	29
February											18	21
Mar									-3.5	-3.5	4	6
April							-21	-16			-11	-10
May					-33.5	-18			-25.5	-19.5	-23.5	-18.5
June											-28.5	-20
July			8	9			-14.5	-12.5	-20.5	-16.5	-24.5	-18.5
August											-15	-13.5
September					18	20			5	6	-2	0
October							22	25			14	16
November									27	29	24	27
December											29	31

north-facing (oriented away from the equator) during the rainy season but south-facing during the dry season.

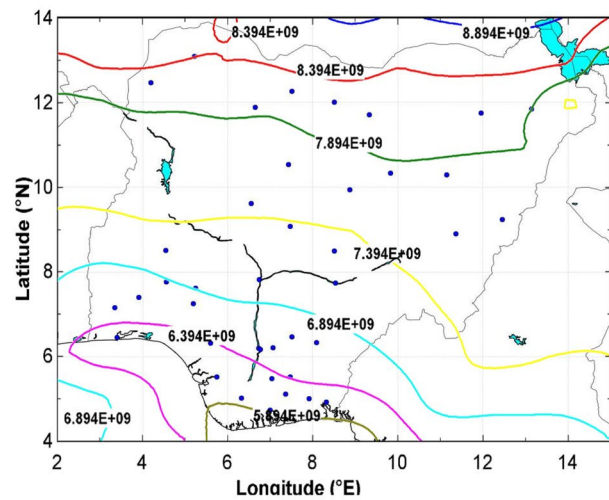
To aid the design and operation of solar collectors, charts of β_{opt} data have been presented for locations in Nigeria for the six tilt adjustment schemes studied. Furthermore, plots of the possible ranges of β_{opt} for the different schemes have also been tabulated. Subsequent collector design steps which rely on these will need to incorporate considerations of temperature effects, wind speed and direction, terrain,

architecture, vegetation, etc., as they specifically affect the particular solar energy conversion application.

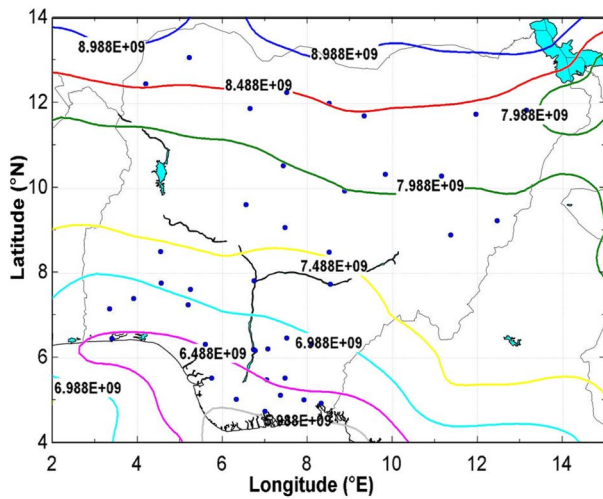
Finally, the obtainable total annual irradiation increases as the number of intermittent adjustments increases. However, of the five periodic adjustment schemes, adjusting three times in the year is recommended as ideal, considering the gains in the obtainable solar energy which it offers compared to the annually fixed collector scheme.



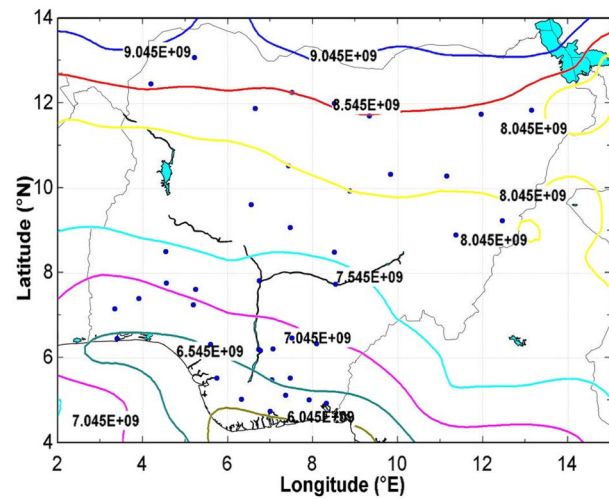
(a) Fixed all year round



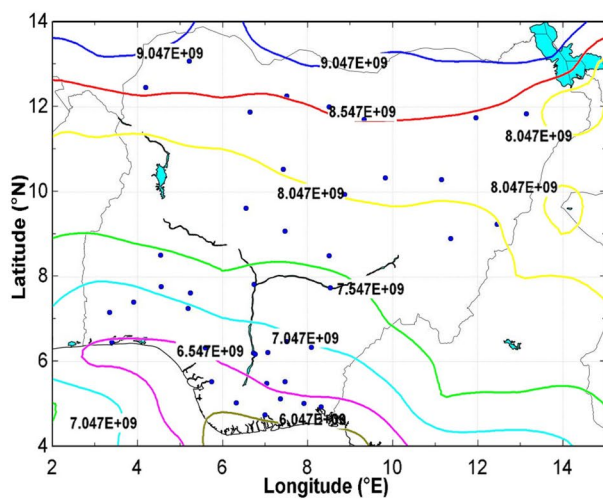
(b) Adjusted two times a year



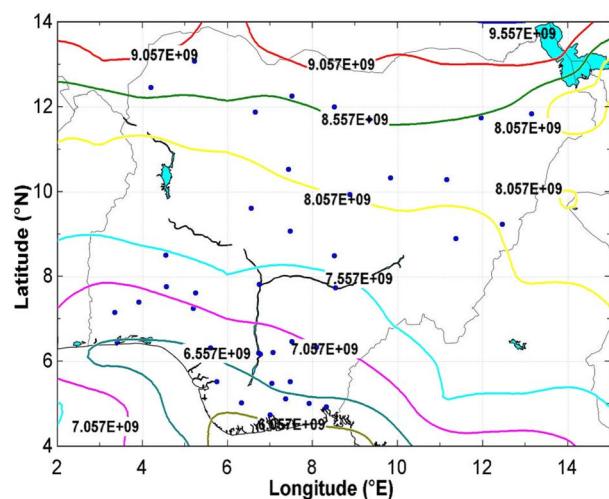
(c) Adjusted three times a year



(d) Adjusted four times a year



(e) Adjusted six times a year



(f) Adjusted twelve times a year

Fig. 12 Available irradiation (J/m^2) on a fixed surfaces and those periodically adjusted **b** twice, **c** thrice, **d** four times, **e** six times, and **f** 12 times in the year

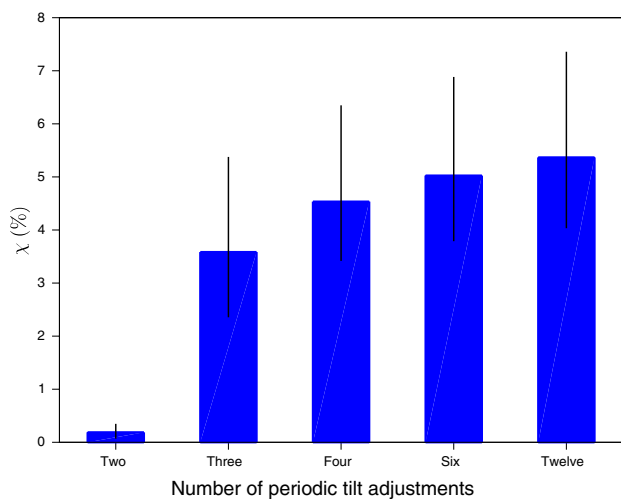


Fig. 13 Comparison of total energy gains under the different schemes with the annual fixed β_{opt} as the base case

Acknowledgements No external funding was received for the study reported in this paper.

References

- Bari, S. (2000). Optimum slope and orientation of solar collectors for different periods of possible utilization. *Energy Conversion and Management*, 41(8), 855–860. [https://doi.org/10.1016/S0196-8904\(99\)00154-5](https://doi.org/10.1016/S0196-8904(99)00154-5).
- Chow, T. T., & Chan, A. L. S. (2004). Numerical study of desirable solar collector orientations for the coastal region of South China. *Applied Energy*, 79, 249–260. <https://doi.org/10.1016/j.apene.2004.01.001>.
- Collares-Pereira, M., & Rabl, A. (1979). The average distribution of solar radiation correlations between diffuse and hemispherical and between daily and hourly insolation values. *Solar Energy*, 22(2), 155–164. [https://doi.org/10.1016/0038-092X\(79\)90100-2](https://doi.org/10.1016/0038-092X(79)90100-2).
- Danandeh, M., & Mousavi, G. S. (2018). Solar irradiance estimation models and optimum tilt angle approaches: A comparative study. *Renewable and Sustainable Energy Reviews*, 92, 319–330. <https://doi.org/10.1016/j.rser.2018.05.004>.
- Despotovic, M., & Nedic, V. (2015). Comparison of optimum tilt angles of solar collectors determined at yearly, seasonal and monthly levels. *Energy Conversion and Management*, 97, 121–131. <https://doi.org/10.1016/j.enconman.2015.03.054>.
- Duffie, J. A., & Beckman, W. A. (2013). *Solar engineering of thermal processes* (4th ed.). New Jersey: Wiley.
- Elminir, H., Ghitas, A., El-Hussainy, F., Hamid, R., Beheary, M., & Abdel-Moneim, K. (2006). Optimum solar flat-plate collector slope: Case study for Helwan. *Egypt Energy Conversion and Management*, 47, 624–637. <https://doi.org/10.1016/j.enconman.2005.05.015>.
- Ghosh, H., Bhowmik, N., & Hussain, M. (2010). Determining seasonal optimum tilt angles, solar radiations on variously oriented, single and double axis tracking surfaces at dhaka. *Renewable Energy*, 35(6), 1292–1297. <https://doi.org/10.1016/j.renene.2009.11.041>.
- Gueymard, C., & Ruiz-Arias, J. (2016). Performance of statistical comparison models of solar energy on horizontal and inclined surface. *Solar Energy*, 128, 1–30. <https://doi.org/10.1016/j.solener.2015.10.010>.
- Ibrahim, D. (1995). Optimum tilt angle for solar collectors used in Cyprus. *Renewable Energy*, 6(7), 813–819. [https://doi.org/10.1016/0960-1481\(95\)00070-Z](https://doi.org/10.1016/0960-1481(95)00070-Z).
- Idowu, O., Olarenwaju, O., & Ifedayo, O. (2013). Determination of optimum tilt angles for solar collectors in low latitude tropical region. *International Journal of Energy and Environmental Engineering*, 4(29), 1–10. <https://doi.org/10.1186/2251-6832-4-29>.
- Kawajiri, K., Oozeki, T., & Genchi, Y. (2011). Effect of temperature on PV potential in the world. *Environmental Science Technology*, 45, 9030–9035. <https://doi.org/10.1021/es200635x>.
- Khoo, Y., Nobre, A., Malhotra, R., Yang, D., Ruther, R., & AG, A. (2014). Optimal orientation and tilt angle for maximizing in-plane solar irradiation for PV applications in Singapore. *IEEE Journal of Photovoltaic*, 4, 647–653. <https://doi.org/10.1109/JPHOT.OV.2013.2292743>.
- Li, D. H. W., & Lam, J. C. (2000). Evaluation of slope irradiance and illuminance models against measured Hong Kong data. *Build Environment*, 35(4), 501–509. [https://doi.org/10.1016/S0360-1323\(99\)00043-8](https://doi.org/10.1016/S0360-1323(99)00043-8).
- Liu, B., & Jordan, R. (1960). The interrelationship and characteristic distribution of direct, diffuse and total solar radiation. *Solar Energy*, 4(3), 1–19.
- Lorenzo, E. (2003). Handbook of Photovoltaic Science and Engineering. In: A. Luque, S. Hegedus (Eds.), *Energy Collected and Delivered by PV Modules* (pp. 905–970). West Sussex: Wiley.
- Morcos, V. H. (1994). Optimum tilt angle and orientation for solar collectors in Assiut. *Egypt Renewable Energy*, 4(3), 291–298. [https://doi.org/10.1016/0960-1481\(94\)90032-9](https://doi.org/10.1016/0960-1481(94)90032-9).
- NASA-SSE (2016) Surface meteorology and solar energy (SSE) release 6.0 methodology, version 3.1. <http://eosweb.larc.nasa.gov/sse/>. Accessed 29 Nov 2016
- Ng, K., Adam, N., Inayatullah, O., & Ab Kadir, M. (2014). Assessment of solar radiation on diversely oriented surfaces and optimum tilts for solar absorbers in Malaysia tropical latitude. *International Journal of Energy and Environment Engineering*, 5(5), 1–13.
- Nijegorodov, N., Devan, K., Jain, P., & Carlsson, S. (1994). Atmospheric transmittance models and an analytical method to predict the optimum slope on an absorber plate, variously oriented at any latitude. *Renewable Energy*, 4(5), 529–543. [https://doi.org/10.1016/0960-1481\(94\)90215-1](https://doi.org/10.1016/0960-1481(94)90215-1).
- Njoku, H. O. (2016). Upper-limit solar photovoltaic power generation: Estimates for 2-axis tracking collectors in Nigeria. *Energy*, 95(15), 504–516. <https://doi.org/10.1016/j.energy.2015.11.078>.
- Noorian, A., Moradi, I., & Kamali, G. A. (2008). Evaluation of 12 models to estimate hourly diffuse irradiation on inclined surfaces. *Renewable Energy*, 33(6), 1406–1412. <https://doi.org/10.1016/j.renene.2007.06.027>.
- Notton, G., & Diaf, S. (2016). Availability solar energy for flat-plate solar collectors mounted on a fixed or tracking structure. *International Journal of Green Energy*, 13(2), 181–190. <https://doi.org/10.1080/15435075.2014.937866>.
- Oladiran, M. T. (1995). Mean global radiation captured by inclined collectors at various surface azimuth angles in Nigeria. *Applied Energy*, 52, 317–330. [https://doi.org/10.1016/0360-2619\(95\)00016-X](https://doi.org/10.1016/0360-2619(95)00016-X).
- Oner, Y., Cetin, E., Yilanci, A., & Ozturk, H. K. (2009). Design and performance evaluation of a photovoltaic sun-tracking system driven by a three-freedom spherical motor. *International Journal of Exergy*, 6(5), 853–867. <https://doi.org/10.1504/IJEX.2009.028578>.
- Perez, R., Ineichen, P., Seals, R., Michalsky, J., & Stewart, R. (1990). Modeling daylight availability and irradiance components from direct and global irradiance. *Solar Energy*, 44(5), 271–289. [https://doi.org/10.1016/0038-092X\(90\)90055-H](https://doi.org/10.1016/0038-092X(90)90055-H).

- Skerker, K. (2009). Optimum tilt angle and orientation for solar collectors in Syria. *Energy Conversion and Management*, *50*, 2439–2448.
- Tang, R., & Wu, T. (2004). Optimal tilt-angles for solar collectors used in china. *Applied Energy*, *79*, 239–248. <https://doi.org/10.1016/j.apenergy.2004.01.003>.
- Yadav, A. K., & Chandel, S. (2013). Tilt angle optimization to maximize incident solar radiation: A review. *Renewable and Sustainable Energy Reviews*, *23*, 503–513. <https://doi.org/10.1016/j.rser.2013.02.027>.
- Yakup, M., & Malik, A. (2001). Optimum tilt angle and orientation for solar collector in brunei darussalam. *Renewable Energy*, *24*(2), 223–234. [https://doi.org/10.1016/S0960-1481\(00\)00168-3](https://doi.org/10.1016/S0960-1481(00)00168-3).
- Yang, D. (2016). Solar radiation on inclined surfaces: Corrections and benchmarks. *Solar Energy*, *136*, 288–302. <https://doi.org/10.1016/j.solener.2016.06.062>.
- Zawilska, E., & Brooks, M. (2011). An assessment of the solar resource for Durban, South Africa. *Renewable Energy*, *36*, 3433–3438. <https://doi.org/10.1016/j.renene.2011.05.023>.